

# An electrophysiological model of the pharyngeal muscle in *Caenorhabditis elegans*

Yuya Hattori<sup>1,2</sup>, Michiyo Suzuki<sup>2</sup>, Zu Soh<sup>3</sup>, Yasuhiko Kobayashi<sup>2</sup>, and Toshio Tsuji<sup>4</sup>

<sup>1</sup> Department of System Cybernetics, Graduate School of Engineering, Hiroshima University, Hiroshima 739-8527, Japan

<sup>2</sup> Quantum Beam Science Directorate, Japan Atomic Energy Agency, Gunma 370-1292, Japan.

<sup>3</sup> Department of Biotechnology, Graduate School of Engineering, Osaka University, Osaka 565-0871, Japan.

<sup>4</sup> Department of Electrical, Systems and Mathematical Engineering, Faculty of Engineering, Hiroshima University,  
Hiroshima 739-8527, Japan

(Tel: 81-27-346-9542, Fax: 81-27-346-9688)

<sup>1</sup> hattori@bsys.hiroshima-u.ac.jp (Hattori, Y.)

**Abstract:** The pharyngeal pumping motion to send food to the bowel is a rhythmic movement in *Caenorhabditis elegans*. We proposed a computer simulation of the pumping motion to investigate the mechanisms of rhythm phenomena in living organisms. To conduct the simulations we developed an electrophysiological model of the pharyngeal muscle that corresponds to the actual structure at a muscular level, and which generates the pumping rhythms. Each of 29 cells was modeled as a membrane potential model to simulate the internal response. The electrophysiological responses of the pharyngeal muscular cells were measured as an electropharyngeogram (EPG) that records the activities of the pharynx as a signal pattern, including the membrane potentials in multiple cells. We also developed an EPG model that calculated EPG based on the outputs of individual membrane-potential models. We confirmed that our model of the pharynx could generate rhythms similar to the EPG measured from *C. elegans*.

**Keywords:** *C. elegans*, electropharyngeogram, electrophysiological model, pharyngeal muscle, pumping motion

## 1 INTRODUCTION

Living organisms exhibit various rhythmic movements such as walking and myocardial pulsation, which are important for their survival. The mechanisms of generation and control of these rhythmic movements remain largely unknown. Further understanding of these mechanisms may help in the treatment of diseases caused by defects in rhythmic control. Further, if the mechanisms can be modeled, they can be applied to engineering systems including developing novel control methods of humanoid robots.

The nematode *Caenorhabditis elegans* is a well-studied model organism with a simple nervous system, and shows several rhythmic movements including the pumping motion for chewing and swallowing involving the pharyngeal muscle. The pharyngeal muscle is composed of only 20 muscular cells and 9 marginal cells. Various biological signals including membrane potentials have been measured in pharyngeal muscular cells using the electropharyngeogram (EPG), and there is evidence that the pumping rhythms are generated by the pharyngeal muscular cells and controlled by pharyngeal neuronal cells (neurons) [1]. In addition, we recently reported that the pumping rhythms temporarily change after ionizing irradiation [2]. Thus, the pumping motion in *C. elegans* is considered a useful system to investigate the mechanisms of rhythmic phenomena in living organisms. However, it is difficult to measure the membrane potentials of individual pharyngeal muscular cells by electrophysiological

techniques, and as such the mechanisms of rhythm generation and control in pharyngeal muscular cells are not well understood.

In the present study, we propose a computer simulation with a mathematical model that is constructed based on the actual structure of the *C. elegans* pharynx, and which corresponds to the biological response at an individual cellular level. A previous study superficially simulated the pharyngeal motion sending food to bowel [3] and is impossible to represent the cell-level responses. Therefore, we propose a structure-based pharyngeal model that can be used for the cell-level analysis and simulation of rhythmic phenomena. The first step of these simulations involves developing a mathematical model of the pharyngeal muscle of *C. elegans* to reproduce the pumping rhythms.

In section 2, we give an outline of the pharyngeal pumping motion and introduce the EPG, which is caused by the electrophysiological responses of muscular cells. In section 3, we model individual cells in the pharynx at the membrane-potential level, and propose a method to tune multiple parameters included in the model comprised of individual muscular-cell models using a genetic algorithm. In section 4, we confirm that an appropriate set of parameters is obtained by our parameter-tuning method and that the model can generate rhythms similar to the EPG measured from *C. elegans*. In section 5, we provide a conclusion to our study and discuss future research.

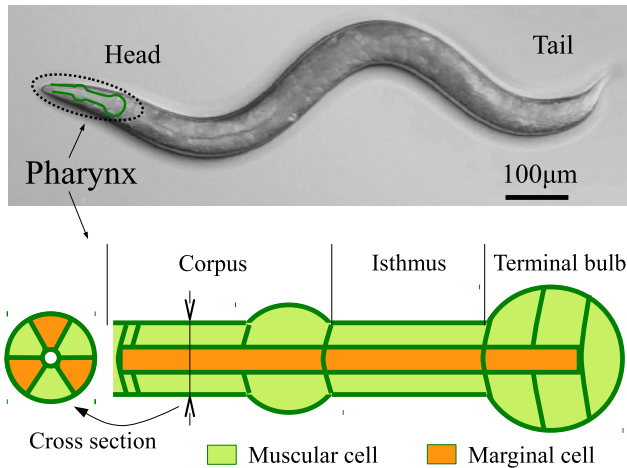


Fig. 1. Structure of the pharyngeal muscle in *C. elegans*.

## 2 PHARYNGEAL MUSCLE IN *C. ELEGANS*

### 2.1 Structure of the pharyngeal muscle

*C. elegans* has a simple cylindrical body approximately 1 [mm] in length (Fig.1, upper panel), and the body is composed of 959 cells. Neuronal networks consisting of 302 neurons include approximately 5,000 chemical synapse connections, approximately 600 gap junctions and approximately 2,000 connections between neurons and muscles [1]. The pumping motion (chewing and swallowing) is a rhythmic movement that is generated by the pharyngeal muscle and is required to send food (bacterial cells) to the bowel. The pharyngeal muscle alternatively contracts and relaxes 0.3 [sec]. It is structurally divided into the corpus, the isthmus and the terminal bulb (Fig.1, lower panel). The corpus is composed of four different types of 10 muscular cells (pm1, pm2VL, pm2VR, pm2D, pm3VL, pm3VR, pm3D, pm4VL, pm4VR and pm4D) and three marginal cells (mc1V, mc1DL and mc1DR). The isthmus is composed of one type of three muscular cells (pm5VL, pm5VR and pm5D) and three marginal cells (mc3V, mc3DL, and mc3DR). The terminal bulb is composed of three different types of seven muscular cells (pm6VL, pm6VR, pm6D, pm7VL, pm7VR, pm7D and pm8) and three marginal cells (mc3V, mc3DL and mc3DR). Muscular cells and marginal cells are alternately arranged in a radial manner (Fig 1, cross-section view). Each marginal cell connects with the adjacent pharyngeal muscular cells by gap junctions and does not contract and relax.

The functions of some pharyngeal neurons in the pumping motion have been elucidated, including the control of the interval between contraction and relaxation of the pharyngeal muscle and control of the pumping cycle. In addition, cell ablation studies have demonstrated that the rhythm of the pumping motion is generated by only pharyngeal muscular cells, as the pumping motion continues after all pharyn-

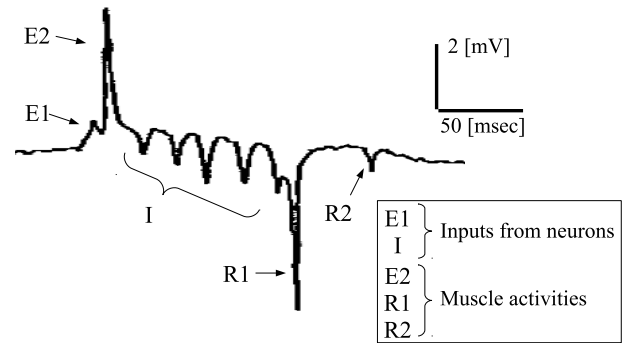


Fig. 2. The EPG recorded by Raizen et al. (revised Fig. 6A in the literature [5]).

geal neurons are killed. Furthermore, the activity of muscular cells in the pharynx is synchronized by signal transduction via gap junctions between muscular cells, as mutants with a defect in the function of the gap junctions in the isthmus show disrupted synchronization between the muscular cell in the corpus and those in the terminal bulb.

### 2.2 Electropharyngeogram (EPG)

Several methods to measure activities of muscular cells in the pharynx have been developed, including membrane-potential recording [4], myoelectric-potential recording [5] and cell imaging [6]. In particular, the myoelectric-potential recording is a popular method that can record the activities of pharyngeal cells as a signal pattern, including the membrane potentials, in the multiple pharyngeal muscular cells. The myoelectric potential in *C. elegans* is termed the electropharyngeogram (EPG). The EPG is measured by fitting a glass electrode into head of a fixed *C. elegans*, and is calculated as the difference of voltages between recordings with and without the pharynx. The EPG is composed of the time derivative of membrane potentials summed over all pharyngeal muscles and the input signals from neurons. Thus, each rapid positive change in membrane potential is observed as a positive spike in the EPG, and vice versa. However, the activity of the peristaltic motion present in the isthmus is not shown in the EPG. Each spike observed in the EPG is termed E1, E2, I, R1 and R2 (Fig. 2). E1 corresponds to the inputs by MC neurons, E2 corresponds to the contraction of the corpus and terminal bulb, I corresponds to the inputs by M3 neurons, R1 corresponds to the relaxation of the corpus and R2 corresponds to the relaxation of the terminal bulb. There is individual variability in the voltage level of the spikes depending on the electrical property of the membrane and/or the measurement environments. Therefore, we focused on the qualitative properties of the EPG including the spiking intervals that are largely independent of individual variance.

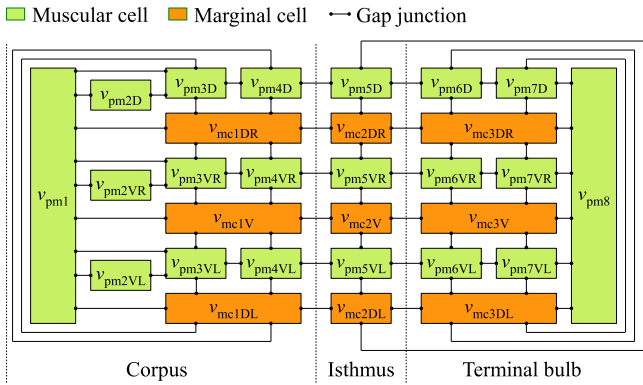


Fig. 3. Electrophysiological model of the pharyngeal muscle.

### 3 ELECTROPHYSIOLOGICAL MODEL OF THE PHARYNGEAL MUSCLE

In this next section, we propose an electrophysiological model of the pharyngeal muscle, which can reproduce the membrane potential of each cell and the EPG of the pharynx. This model is composed of two parts; a membrane potential model of individual cells in the pharynx (cell-level model) and an EPG model to reproduce the EPG based on the outputs of membrane potential models. The parameters of the membrane-potential models are then tuned to reproduce the actual EPG.

#### 3.1 Membrane potential model (cell-level model)

The membrane potential of each pharyngeal muscular cell in the pharynx is important for the rhythm generation and synchronization in the pumping motion [7]. Therefore, we developed a mathematical model of each cell that shows the cell response at the membrane-potential level. Based on the actual structure of *C. elegans* [1], [8], we utilized all 29 cells in the pharynx (i.e., 20 muscular cells and 9 marginal cells), and modeled each of them individually. In the model of the cell  $n (\in \text{pm1}, \text{pm2VL}, \dots, \text{mc3DR})$ , the membrane potential is represented by  $v_n$  (Fig. 3). To describe the behavior of  $v_n$ , we introduced the FitzHugh-Nagumo model [9], [10], which is used for heart muscle modeling and analyses of various rhythmic phenomena. Cells,  $n$  and  $m$ , are connected by gap junctions based on the actual structure [8], and the connection weight is represented by  $w_{n,m}$ . Note that  $w_{m,n} = w_{n,m}$ . The electrical current from  $m$  to  $n$  is given by  $w_{n,m}(v_m - v_n)$  using  $w_{n,m}$  and the difference of potential between  $v_m$  and  $v_n$ . Therefore, the membrane potential,  $v_n$ , is represented by:

$$T_n \frac{dv_n}{dt} = c_n \left\{ v_n - \frac{v_n^3}{3} - u_n + \sum_m w_{n,m}(v_m - v_n) \right\}, \quad (1)$$

$$T_n \frac{du_n}{dt} = \frac{1}{c_n} (a_n + v_n - b_n u_n), \quad (2)$$

where  $T_n$  is a time constant to account for the rapid change of the membrane potential in the pumping motion.  $a_n$ ,  $b_n$ , and  $c_n$  are constants used in the FitzHugh-Nagumo model.  $u_n$  is a recovery variable. These parameters determine the cycle and the response rate of  $v_n$ , and should be tuned to generate rhythms in the pumping motion. This is the first model to reproduce the activities of individual cells in the pharynx at the membrane potential level.

Since the EPG can be used to directly observe the rhythms generated in the pharynx, we used the EPG to compare the rhythm of  $v_n$  with that of the pumping motion itself. For this purpose, we developed the EPG model to calculate the EPG based on the individual membrane potential models.

#### 3.2 EPG model

We calculated the EPG based on the membrane potential,  $v_n$ , of each cell model in 3.1. The EPG is measured as the time derivative of the membrane potentials summed over all pharyngeal muscular cells because there is a capacitance between the electrode and the head of the *C. elegans*. Therefore, the EPG,  $V_{\text{model}}^{\text{EPG}}$ , generated by  $v_n (n \in \text{pm1}, \text{pm2D}, \dots, \text{mc3V})$  is represented by:

$$V_{\text{model}}^{\text{EPG}} = \sum_n R_n C \frac{dv_n^{\text{act}}}{dt}, \quad (3)$$

$$v_n^{\text{act}} = \max(v_n, 0), \quad (4)$$

where  $v_n^{\text{act}} (n \in \text{pm1}, \text{pm2D}, \dots, \text{mc3V})$  is an action potential,  $R_n$  is a resistance depending on the distance between the electrode and the cell body, and  $C$  is a capacitance. We can compare the rhythm of  $v_n$  with that of the pumping motion by using the EPG model.

#### 3.3 Parameter tuning method for the pharyngeal muscle model

The parameters should be well tuned in order to reproduce the actual EPG using the model. To tune parameters included in the membrane potential model of each cell in 3.1, we compared the actual EPG recorded from a *C. elegans* with the EPG calculated by the model in 3.2. As the recorded EPG is affected by electrical properties of the membrane and/or measurement environments, there is individual variability in the voltage level of the spikes. Therefore, we used qualitative properties, in particular spiking intervals, which are largely independent of individual variability, for the parameter tuning. The spikes that correspond to muscular activities are E2, R1, and R2 (Fig. 2). Positive and negative membrane potentials in the corpus cells generate E2 and R1 spikes, respectively, while positive and negative membrane potentials in the terminal-bulb cells generate E2 and R2 spikes, respectively. Therefore, we tuned the membrane potential models

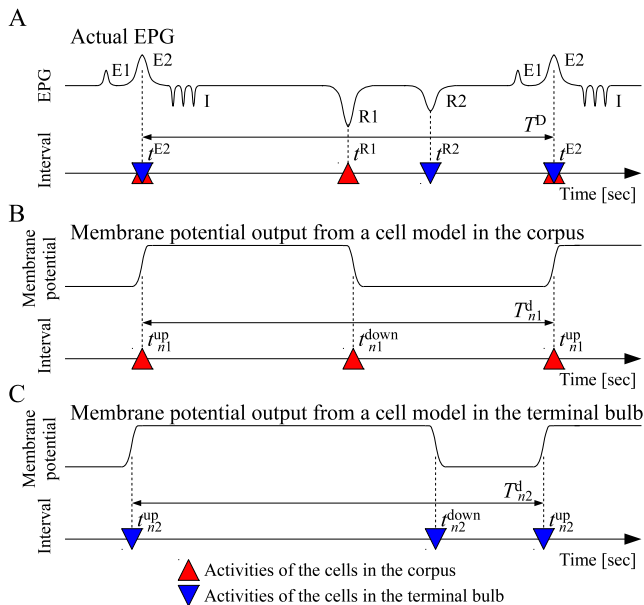


Fig. 4. Intervals of the activities of the corpus and the terminal bulb.

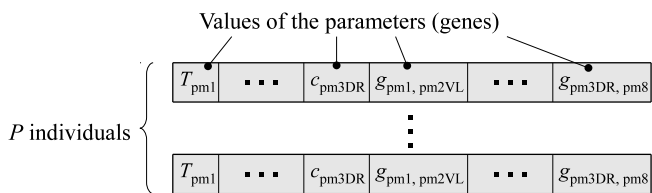


Fig. 5. The GA string.

to reflect the positive and negative membrane potential properties and the spiking intervals between each spike in the actual EPG.

$t^{E2}$ ,  $t^{R1}$ , and  $t^{R2}$  represent the intervals of E2, R1, and R2 (Fig. 4A), and are calculated as the peak value of each spike. In addition, the pumping cycle measured from the actual EPG is represented by  $T^D$ . The positive and negative intervals in the outputs of the membrane potential models in the corpus are represented by  $t_{n1}^{up}$  and  $t_{n1}^{down}$  (Fig. 4B), where  $n1$  is the cell name (pm1, pm2VL, pm2VR, pm2D, pm3VL, pm3VR, pm3D, pm4VL, pm4VR, pm4D, mc1V, mc1DL, and mc1DR). The positive and negative intervals in the outputs of the membrane potential models in the terminal bulb are represented by  $t_{n2}^{up}$  and  $t_{n2}^{down}$  (Fig. 4C), where  $n2$  is the cell name (pm6VL, pm6VR, pm6D, pm7VL, pm7VR, pm7D, pm8, mc3V, mc3DL, and mc3DR). These parameters are calculated as the maximum/minimum values of the time derivative of each membrane potential model. In addition, the output cycles of the membrane potential models of the corpus and the terminal bulb are represented by  $T_{n1}^d$  and  $T_{n2}^d$ , respectively.

To evaluate the fitness of the positive and negative intervals calculated by the individual membrane potential models of the pharyngeal cells, we defined the following error judgment standard that compares the intervals of membrane potentials output from individual cell models to the actual EPG in the pharynx:

$$E = \frac{E^c + E^t}{23}, \quad (5)$$

$$E^c = \sum_{n1} \frac{|t^{E2} - t_{n1}^{up}| + |t^{R1} - t_{n1}^{down}| + |T^D - T_{n1}^d|}{3}, \quad (6)$$

$$E^t = \sum_{n2} \frac{|t^{E2} - t_{n2}^{up}| + |t^{R2} - t_{n2}^{down}| + |T^D - T_{n2}^d|}{3}, \quad (7)$$

where  $E^c$  is an integrating error of the corpus cells, and  $E^t$  is an integrating error of the terminal bulb cells. As the activity of the isthmus cells is not shown in the actual EPG, we evaluated the fitness of 23 membrane potential models in the isthmus (6 membrane potential models were not used). The smaller the  $E$ , the more the EPG model reproduces the actual EPG. We employed a learning and evolutionary genetic algorithm (GA) to suitably tune the parameters included in the membrane potential models on the basis of  $E$ .

First, all the parameters included in the membrane potential models are represented as individual genes in a GA string (Fig. 5). A string arranging all the parameters (genes) is treated as an individual in the GA.  $P$  individuals are produced, where the initial value for each gene is given as a uniform random number. Next, all individuals of the current generation (the repeat number of calculation for the GA tuning) are evaluated by equation (5), which are used to produce the next generation. The elite  $R_{elite}$  [%] individuals with the superior error value,  $E$ , remain as a part of the next generation.  $(100 - R_{elite})$  [%] of the population of the next generation is produced by the three operations of a GA; i.e., crossover for  $R_{crossover}$  [%] of the population, mutation for  $R_{mutation}$  [%] of the population, and copying for  $R_{copying}$  [%] of the population. These procedures (evaluation, crossover, mutation, copying) are repeated every generation until the generation  $g$  reaches  $G$ . We essentially follow the procedures of GA operations we previously reported [11].

## 4 REPRODUCTION OF PUMPING RHYTHMS

### IN A WILD TYPE *C. ELEGANS*

We evaluated the effectiveness of our proposed pharyngeal muscle model. To generate the actual pumping rhythms in our model, we tuned the parameters included in the membrane potential models by the GA-based tuning method. As an example to reproduce the actual EPG, we used the EPG of a wild type *C. elegans* in which neurons except for the M4 neuron were ablated.

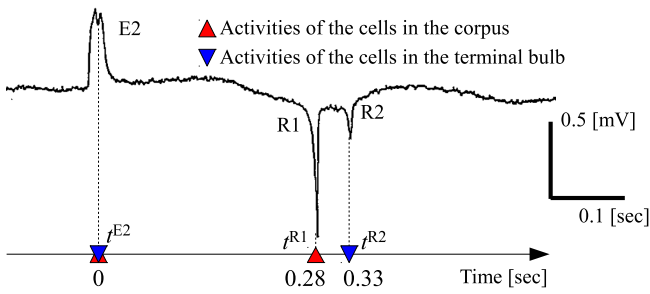


Fig. 6. EPG measured by Raizen et al. (revised Fig. 6A in the literature [5]).

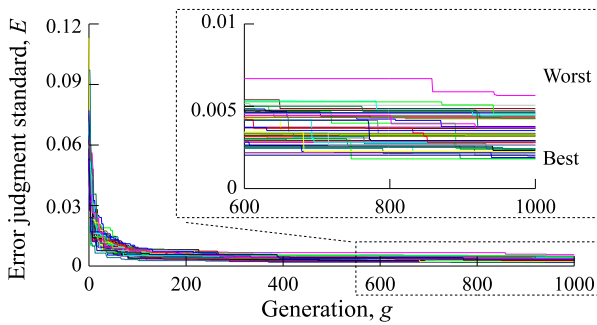


Fig. 7. Evolution of the error judgment standard,  $E$ .

#### 4.1 Methods

The EPG includes E1 and I spikes corresponding to neuronal activity and E2, R1, while R2 spikes correspond to muscular activity. As the proposed electrophysiological model targets only muscular activity, we employed the EPG measured from a wild type *C. elegans* in which all neurons but the M4 neuron were ablated [5]. As shown in Fig.6, the EPG includes only E2, R1, and R2 spikes. Although the M4 neuron controls the peristaltic motion of the isthmus, the input from the M4 neuron to the pharyngeal muscle and the peristaltic motion are not shown in the EPG. Therefore, the spikes observed in Fig.6 can be treated as muscular activity only.

The data of the spiking intervals used for the parameter-tuning were derived from the EPG in Fig.6, where we defined the spiking interval of E2 as a standard time ( $t^{E2} = 0$  [sec]) and the spiking intervals of R1 and R2 were given by  $t^{R1} = 0.28$  [sec] and  $t^{R2} = 0.33$  [sec], respectively. The pumping cycle was given by  $T^D = 1.2$  [sec]. The spiking intervals calculated by the membrane potential models,  $t_n^{up}$  and  $t_n^{down}$ , were normalized by those generated by a cell near the glass electrode, pm4D ( $t_{pm4D}^{up} = 0$  [sec]). The range of parameters used in this simulation were  $T_n = [0, 0.1]$ ,  $a_n = [0, 1]$ ,  $b_n = [0, 1]$ ,  $c_n = [0, 10]$ , and  $w_{n,m} = [0, 1]$ . Parameters included in the models of the same types of cells are tuned as the same value. The condition settings of the GA were set to  $P =$

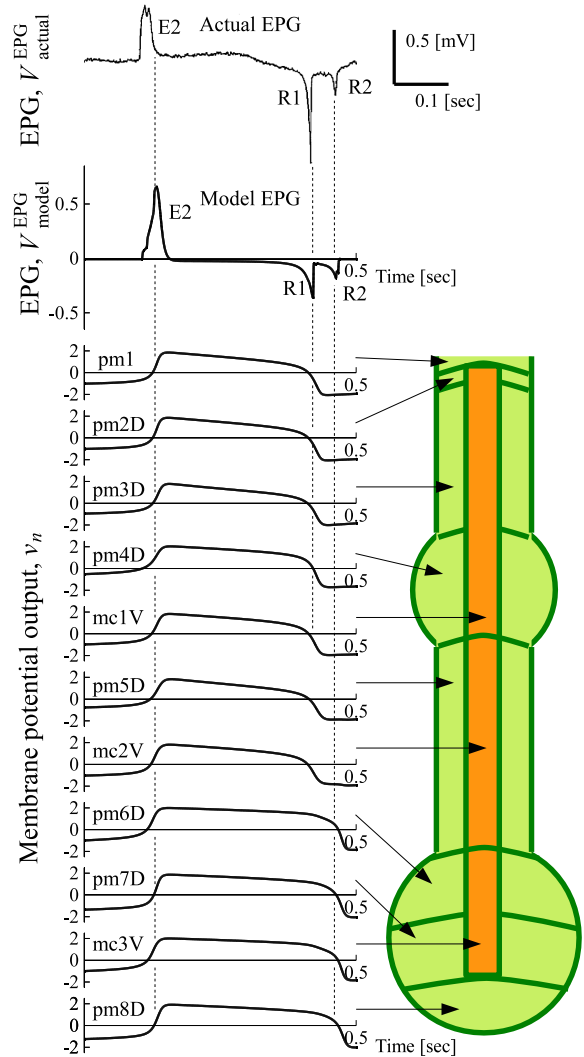


Fig. 8. Reproduction of pumping rhythms of a wild type *C. elegans* at the EPG level.

20,  $R_{elite} = 5$ ,  $R_{crossover} = 76$  [%],  $R_{mutation} = 9.5$  [%],  $R_{copying} = 9.5$  [%], and the at-end generation was set to  $G = 1,000$ .

#### 4.2 Results

We conducted 50 trials using different initial values for the GA-based tuning method. Evolution of the error judgment standard,  $E$ , in a top individual at each GA generation among 50 trials is shown in Fig. 7. Values of  $E$  among all trials decreased rapidly until  $g = 100$ , and were less than  $E = 0.015$  at  $g \leq 200$ . After  $g = 200$ , values of  $E$  among all trials decreased slowly, and at  $g = 1,000$  the maximal and minimal values reached  $E = 0.0056$  and  $E = 0.0018$ , respectively (worst and best trials in Fig. 7).

The membrane potential output of individual cell models,  $v_n$ , employing a set of the parameters obtained at  $g = 1,000$  and the EPG,  $V_{model}^{EPG}$ , calculated from  $v_n$  are shown in Fig. 8.

The output EPGs from the actual *C. elegans* and the proposed model,  $V_{\text{actual}}^{\text{EPG}}$  and  $V_{\text{model}}^{\text{EPG}}$ , are shown on the top panel.  $V_{\text{actual}}^{\text{EPG}}$  is a replot of Fig. 6. The EPG of the model was calculated based on  $v_n$  of the membrane potential models of 23 cells (equations (3) and (4)). Since the cells in the pharynx are divided into 11 types based on the function, a single example of output of each is shown on the bottom panel. The right panel shows the position of each cell in the pharynx. The capacitance included in equation (3) was set to  $C = 276$  [pF] based on a previous report [4]. The resistances included in equation (3) were set to  $R_{\text{pm4VL}} = R_{\text{pm4VR}} = R_{\text{pm4D}} = 1$  [M $\Omega$ ] and  $R_{\text{pm6VL}} = R_{\text{pm6VR}} = R_{\text{pm7D}} = R_{\text{pm7VR}} = R_{\text{pm7D}} = 0.3$  [M $\Omega$ ]. The resistances corresponding to the isthmus were set to  $R_n = 0$  [M $\Omega$ ] as the activity of the cells in the isthmus is not shown in the actual EPG. Other resistances were set to  $R_n = 0.01$  [M $\Omega$ ]. From Fig. 8, we confirmed that the shapes of the membrane potential,  $v_n$ , were similar in all cells. In the membrane potential models of all cells, the rising time of  $v_n$  is the same as that of the spike E2 in the actual EPG.  $v_n$  in the corpus decreased corresponding to the decrease of the spike R1, and  $v_n$  in the terminal bulb decreased at the same time as R2 in the actual EPG. Furthermore, the EPG of the proposed model,  $V_{\text{model}}^{\text{EPG}}$ , calculated based on  $v_n$ , was similar to the actual EPG,  $V_{\text{actual}}^{\text{EPG}}$ . As such, the proposed electrophysiological model of the pharyngeal muscle composed of the membrane potential models accurately reproduced the pumping rhythms (i.e., spiking intervals of the actual EPG).

## 5 CONCLUSION

In this paper, we developed a membrane potential model of individual muscular cells in the pharynx based on the actual structure of the *C. elegans* to investigate the mechanisms of rhythm generation and control in living organisms. In addition, we proposed an EPG-level model that calculates the electropharyngeogram (EPG) based on outputs of individual membrane potential models. In the parameter tuning for the membrane potential models, we focused on the spiking intervals in the actual EPG and tuned the parameters so as to reproduce the intervals rather than the EPG itself. In our numerical experiment of rhythm generation, the proposed model successfully generated similar pumping rhythms to those observed in a wild type *C. elegans*.

As our model was based on the actual structure of cell connections and each cell corresponds to the actual cell in the *C. elegans*, by ablating each connection included in this model virtually, we can investigate the role of the gap junctions on the rhythmic phenomena. In pilot experiments, we virtually ablated gap junctions in the isthmus, as seen in the *eat-5* mutant that exhibits functional gap junctions deficits in the isthmus and shows disrupted synchronization between

the muscular cells in the corpus and those in the terminal bulb. Similarly, we found that the membrane potential models generated rhythms that were not synchronized between the corpus and the terminal bulb (data not shown). Thus, this model will be useful for further studies examining mechanisms of rhythmic phenomena in *C. elegans*.

## ACKNOWLEDGMENT

This study was partially supported by a Grant-in-Aid for Scientific Research on Innovative Areas from MEXT to T.T. (No. 20115010).

## REFERENCES

- [1] White, J.G., Southgate, E., Thomson, J.N., and Brenner, S. (1986), The structure of the nervous system of the nematode *Caenorhabditis elegans*. Philos. Trans. R. Soc. Lond. B. Biol. Sci. 314, pp. 1-340.
- [2] Suzuki, M., Sakashita, T., Hattori, Y., Tsuji, T., and Kobayashi, Y. (2011), Effects of ionizing radiation on pharyngeal pumping in *Caenorhabditis elegans*. 18th Int. *C. elegans* Meeting, Full Abstracts, pp. 158-159.
- [3] Avery, L. and Shtonda, B.B. (2003), Food transport in the *C. elegans* pharynx. J. Exp. Biol., 206, pp. 2441-2457.
- [4] Shtonda, B. and Avery, L. (2005), CCA-1, EGL-19 and EXP-2 currents shape action potentials in the *Caenorhabditis elegans* pharynx. J. Exp. Biol., 208, pp. 2177-2190.
- [5] Raizen, D.M. and Avery, L. (1994), Electrical activity and behavior in the pharynx of *Caenorhabditis elegans*. Neuron, 12, pp. 483-495.
- [6] Kerr, R., Lev-Ram, V., Baird, G., Vincent, P., Tsien, R.Y., and Schafer, W.R. (2000), Optical imaging of calcium transients in neurons and pharyngeal muscle of *C. elegans*. Neuron, 26, pp. 583-594.
- [7] Starich, T.A., Lee, R.Y.N., Panzarella, C., Avery, L., and Shaw, J.E. (1996), *eat-5* and *unc-7* represent a multigene family in *Caenorhabditis elegans* involved in cell-cell coupling. J. Cell Biol., 134, pp. 537-548.
- [8] Albertson, D.G. and Thomson J.N. (1976), The pharynx of *Caenorhabditis elegans*. Phil. Trans. Roy. Soc. B, 275, pp. 299-325.
- [9] Fitzhugh, R. (1961), Impulses and physiological states in theoretical models of nerve membrane. Biophys. J., 1, pp. 445-466.
- [10] Nagumo, J., Arimoto, S., and Yoshizawa, S. (1961), An active pulse transmission line simulating nerve axon. Proceedings of the IRE, 50, pp. 2061-2070.
- [11] Hattori, Y., Suzuki, M., Soh, Z., Kobayashi, Y., and Tsuji, T. (2012), Theoretical and evolutionary parameter tuning of neural oscillators with a double-chain structure for generating rhythmic signals. Neural Comp., 24, in press.